Can a satellite-derived estimate of the fraction of PAR absorbed by chlorophyll ($FAPAR_{chl}$) improve predictions of light-use efficiency and ecosystem photosynthesis for a boreal aspen forest?

Qingyuan Zhang, Elizabeth. M. Middleton, Hank A. Margolis, Guillaume G. Drolet, Alan A. Barr and T. Andy Black

Gross primary production (GPP) is a key terrestrial ecophysiological process that links atmospheric composition and vegetation processes. Study of GPP is important to global carbon cycles and global warming. One of the most important of these processes, plant photosynthesis, requires solar radiation in the 0.4–0.7 μm range (also known as photosynthetically active radiation or PAR), water, carbon dioxide (CO_2), and nutrients. A vegetation canopy is composed primarily of photosynthetically active vegetation (PAV) and non-photosynthetic vegetation (NPV; e.g., senescent foliage, branches and stems). A green leaf is composed of chlorophyll and various proportions of nonphotosynthetic components (e.g., other pigments in the leaf, primary/secondary/ tertiary veins, and cell walls). The fraction of PAR absorbed by whole vegetation canopy ($FAPAR_{canopy}$) has been widely used in satellite-based Production Efficiency Models to estimate GPP (as a product of $FAPAR_{canopy}$ x PAR x LUE_{canopy}, where LUE_{canopy} is light use efficiency at canopy level). However, only the PAR absorbed by chlorophyll (a product of $FAPAR_{chl}$ x PAR) is used for photosynthesis. Therefore, remote sensing driven biogeochemical models that use $FAPAR_{chl}$ in estimating GPP (as a product of $FAPAR_{chl}$ x PAR x LUE_{chl}) are more likely to be consistent with plant photosynthesis processes.

Our paper has been designed to test which group ([$FAPAR_{canopy}$, LUE_{canopy}] vs. [$FAPAR_{chl}$, LUE_{chl}]) is more consistent with plant photosynthesis processes.

Using a coupled canopy-leaf radiative transfer model, we have estimated $FAPAR_{chl}$ and $FAPAR_{canopy}$ for the Southern Old Aspen forest (SOA) in Canada for 2001-2005 with MODIS images. The tower fluxes over the SOA site provide real time photosynthesis of the forest. The scientists of the SOA site offer the measurements of photosynthesis and their flux tower based LUE (LUE_{tower}). Our results showed that LUE_{chl} matched well with LUE_{tower} both at magnitude and at phase while LUE_{canopy} did not. Using $FAPAR_{canopy}$ to estimate absorbed PAR for photosynthesis will significantly overestimate. One can't get good estimate of GPP phenology if using the group of $FAPAR_{canopy}$ and LUE_{canopy} to estimate GPP. Using $FAPAR_{chl}$ and LUE_{chl} to estimate GPP will get more consistent results and will help the study of global carbon cycles and global warming.

Can a satellite-derived estimate of the fraction of PAR absorbed by chlorophyll ($FAPAR_{chl}$) improve predictions of light-use efficiency and ecosystem photosynthesis for a boreal aspen forest?

Qingyuan Zhang[a,b], Elizabeth M. Middleton[b], Hank A. Margolis[c], Guillaume G. Drolet[c], Alan A. Barr[d] and T. Andrew Black[e]

[a]Goddard Earth Sciences & Technology Center, University of Maryland, Baltimore County, Baltimore, Maryland 21228, USA

[b]Biospheric Sciences Branch, Code 614.4, NASA/Goddard Space Flight Center, Greenbelt, Maryland 20771, USA

[c]Centre d'Étude de la Forêt (CEF), Faculté de Foresterie et de Géomatique, Pavillon Abitibi-Price, Université Laval, Québec City, Québec, Canada G1K 7P4

[d]Atmospheric Sciences and Technology Directorate, Meteorological Service of Canada, Saskatoon, Saskatchewan S7N 3H5 Canada

[e]Biometeorology and Soil Physics Group, 121-2357 Main Mall, University of British Columbia, Vancouver, BC, Canada V6T1Z4

Corresponding author:

Qingyuan Zhang

Address:

Building 33, Room G321
Biospheric Sciences Branch, Code 614.4,
NASA/Goddard Space Flight Center,
Greenbelt, Maryland 20771, USA

Tel: 301-614-6672
Email: qyz72@yahoo.com

Abstract

We used daily MODerate resolution Imaging Spectroradiometer (MODIS) imagery obtained over a five-year period to analyze the seasonal and inter-annual variability of the fraction of absorbed photosynthetically active radiation (FAPAR) and photosynthetic light use efficiency (LUE) for the Southern Old Aspen (SOA) flux tower site located near the southern limit of the boreal forest in Saskatchewan, Canada. To obtain the spectral characteristics of a standardized land area to compare with tower measurements, we scaled up the nominal 500 m MODIS products to a 2.5 km x 2.5 km area (5x5 MODIS 500 m grid cells). We then used the scaled-up MODIS products in a coupled canopy-leaf radiative transfer model, PROSAIL-2, to estimate the fraction of absorbed photosynthetically active radiation (APAR) by the part of the canopy dominated by chlorophyll ($FAPAR_{chl}$) versus that by the whole canopy ($FAPAR_{canopy}$). Using the additional information provided by flux tower-based measurements of gross ecosystem production (GEP) and incident PAR, we determined 90-minute averages for APAR and LUE (slope of GEP:APAR) for both the physiologically active foliage ($APAR_{chl}$, LUE_{chl}) and for the entire canopy ($APAR_{canopy}$, LUE_{canopy}).

The flux tower measurements of GEP were strongly related to the MODIS-derived estimates of $APAR_{chl}$ ($r^2 = 0.78$) but only weakly related to $APAR_{canopy}$ ($r^2 = 0.33$). Gross LUE between 2001 and 2005 for LUE_{chl} was 0.0241 μmol C μmol^{-1} PPFD whereas LUE_{canopy} was 36% lower. Time series of the 5-year normalized difference vegetation index (NDVI) were used to estimate the average length of the core growing season as days of year 152 – 259. Inter-annual variability in the core growing season LUE_{chl} (μmol C μmol^{-1} PPFD) ranged from 0.0225 in 2003 to 0.0310 in 2004. The five-year time series of LUE_{chl} corresponded well with both the seasonal phase and amplitude of LUE from the tower measurements but this was not the case for

LUE_{canopy}. We conclude that LUE_{chl} derived from MODIS observations could provide a more physiologically realistic parameter than the more commonly used LUE_{canopy} as an input to large-scale photosynthesis models.

Key Words: MODIS; aspen; chlorophyll; ecosystem flux; gross primary production; gross ecosystem production; light use efficiency (LUE); LUE_{chl}; $FAPAR_{chl}$; NDVI; LUE_{tower}

1. Introduction

1.1 Background – Using Light Use Efficiency to Estimate Ecosystem Photosynthesis

Realistic models of plant canopy photosynthesis are necessary for obtaining accurate estimates of the carbon cycle for use in land surface models (LSMs) and atmospheric general circulation models (GCMs) (Sellers *et al.* 1996a, 1996b). In vegetative canopies, photosynthetically active radiation (PAR) is absorbed from sunlight by photosynthetic pigments, primarily chlorophyll *a* and its accessory pigments (chlorophyll *b*, carotenoids). When ecosystem photosynthesis is calculated with a process model, it is referred to as Gross Primary Production (GPP). When it is calculated from flux tower data, it is referred to as Gross Ecosystem Production, designated here as GEP_{tower}.

Plant production efficiency models (PEMs) have been developed to estimate GPP at canopy, landscape, regional and global scales, utilizing optical remote sensing to provide the fraction of absorbed PAR (FAPAR). Examples include GLO-PEM (Prince *et al.* 1995, 2000; Prince and Goward 1995, 1996), TURC (Ruimy *et al.* 1994, 1996a, 1996b), 3-PG (Landsberg and Waring 1997; Law *et al.* 2000) and PSN (Running *et al.* 1994, 1999a, 1999b, 2000, 2004). This latter model is a satellite-based global photosynthesis product derived from the MODerate resolution Imaging Spectroradiometer (MODIS) on the Terra and Aqua platforms.

All of these models estimate GPP as the product of three terms: the light use efficiency of the canopy (LUE_{canopy}), which is a measure of the PAR conversion efficiency into photosynthetically fixed CO_2; the FAPAR of the canopy ($FAPAR_{canopy}$), which is estimated using radiative transfer models and remote sensing data or using empirical relationship between $FAPAR_{canopy}$ and the normalized difference vegetation index (NDVI, Tucker 1979); and the incident PAR where:

$$GPP = LUE_{canopy} * FAPAR_{canopy} * PAR. \quad (1)$$

Consequently, accurate estimates of FAPAR and LUE for ecosystems are essential for obtaining accurate GPP.

The LUE concept was initially developed for agricultural crops at harvest to determine the conversion efficiency of available light into biomass (g C dry mass) over a full growing season and is typically expressed in units such as g C MJ^{-1} PAR (Monteith 1972, 1977). This seasonal crop-level LUE represents a direct measure of the average conversion efficiency of all above ground plant material (Gower et al. 1999), which is dominated by foliage for agricultural crops. Eddy covariance flux towers have the capability to provide near-continuous measurements of GEP - denoted as GEP_{tower}, and absorbed PAR - denoted as $APAR_{tower}$ (see section 3.2.3 for more details, also see Krishnan et al., 2006), for an entire ecosystem for time periods as short as 30 minutes. Consequently, these instrumented flux towers also provide near-continuous measurements of LUE, denoted as LUE_{tower}, over these same time periods as:

$$LUE_{tower} = \frac{GEP_{tower}}{FAPAR_{tower} * PAR_{tower}} = \frac{GEP_{tower}}{APAR_{tower}}. \quad (2)$$

The LUE_{tower} is typically expressed as μmol CO_2 μmol^{-1} PAR or μmol C μmol^{-1} PPFD, where PPFD is the photosynthetic photon flux density. For these tower-based calculations, incident PAR is measured directly by radiometers attached to the flux tower and the FAPAR estimate is based both on detailed canopy structural measurements and on the radiometer measurements (Barr et al. 2007). An underlying assumption supporting the LUE retrieval through the MODIS modeling approach is that the LUE_{canopy} used in the models is a good approximation of LUE_{tower}, at least when the measurement footprint of the tower is roughly equivalent to the area of the remote sensing pixel. Apparent ecosystem LUE obtained from flux tower measurements (i.e.,

LUE_{tower}) directly describes the integrated response of the whole ecosystem to the prevailing environmental conditions, as do remotely acquired spectral snapshots although these latter are limited to specific acquisition times and viewing configurations.

On a canopy or ecosystem scale, GEP and APAR are typically linearly related (e.g., Waring et al., 1995), so that LUE can be determined from the slope of this relationship. This apparent linearity results from multiple scattering within the canopy, which involves 3-D contributions from foliage of multiple species and illumination conditions, as well as non-photosynthetic material (e.g., limbs, trunks, cones, litter). On the other hand, comparable light response curves for individual leaves of selected species yield non-linear responses for which the initial slope of the linear portion of the curve describes the quantum efficiency (Mohr et al., 1995). The quantum efficiency of individual leaves can also serve as an input to carbon cycle models but a means of scaling it to the canopy level is still required.

A common modeling approach is to set a maximum LUE for optimal environmental conditions (i.e., unstressed vegetation) and to simulate ecosystem responses when unfavorable environmental conditions occur (e.g., limitations of temperature, humidity, soil moisture, etc.) through down-regulation of the maximum LUE to achieve an apparent LUE (Medlyn, 1998).

The MODIS GPP product, an output of the PSN model, has been compared with measurements made at flux towers by several research groups. For instance, Turner and colleagues (Turner *et al.* 2003, 2004, 2006) found that the annual MODIS GPP totals calculated using MODIS standard photosynthesis products for a deciduous forest in Massachusetts, USA, matched well with the annual GEP totals from the flux tower. However, the seasonal time course of MODIS GPP dynamics differed significantly from the GEP measured by the flux tower

(GEP_{tower}) suggesting that a more physiologically realistic method of estimating GPP could be useful.

1.2 Chlorophyll-based LUE (LUE_{chl})

Even though maximum leaf LUE can be strongly influenced by leaf chlorophyll concentration (e.g., Waring et al. 1995), it is less clear how canopy chlorophyll concentration might influence apparent LUE at the ecosystem scale. Laboratory studies (Yoder and Waring 1994) have shown that variation in canopy total chlorophyll content of miniature Douglas fir canopies was significantly correlated with their photosynthesis, although the correlation was higher for canopies exposed to full sun. Several other studies have shown a relationship between leaf or canopy nitrogen concentration and light use efficiency at the ecosystem scale (Kergoat et al. 2008, Ollinger et al. 2008), However, we believe that remote sensing techniques that evaluate chlorophyll rather than nitrogen could have even greater potential for estimating ecosystem light use efficiency and GPP.

From a biochemical perspective, only the PAR absorbed by photosynthetic pigments (designated as $APAR_{chl}$) enables photosynthetic processes, whereas the PAR absorbed by non-photosynthetic components such as boles, branches, stems, and litter is not used for CO_2 fixation. We designate chlorophyll-based FAPAR here as $FAPAR_{chl}$. By definition, $APAR_{canopy}$ (the product of $FAPAR_{canopy}$ and PAR) is greater than $APAR_{chl}$ (the product of $FAPAR_{chl}$ and PAR). For linking to remote sensing applications, estimates of $APAR_{chl}$ should provide more realistic GEP_{tower} and LUE_{tower} values than similar estimates using $APAR_{canopy}$. We define LUE based on $APAR_{chl}$ versus $APAR_{canopy}$ as follows:

$$LUE_{chl} = \frac{GEP_{tower}}{FAPAR_{chl} * PAR} = \frac{GEP_{tower}}{APAR_{chl}}. \quad (3)$$

$$LUE_{canopy} = \frac{GEP_{tower}}{FAPAR_{canopy} * PAR} = \frac{GEP_{tower}}{APAR_{canopy}}. \quad (4)$$

In earlier studies (Zhang *et al.*, 2005, 2006), an approach to estimate $FAPAR_{chl}$ was proposed using daily MODIS data. Since then, we have refined our algorithm to retrieve $FAPAR_{chl}$ from MODIS imagery using the modified PROSPECT-SAIL2 model, PROSAIL-2 (Zhang *et al.* 2005, 2006). The new version of this algorithm provides a statistical distribution of likely $FAPAR_{chl}$ values for each cloud-free MODIS observation.

In this article, we combine five years of flux, meteorological, and remote sensing data from a boreal aspen flux site to attain the following four objectives: (1) to present a method for estimating $FAPAR_{chl}$ and $FAPAR_{canopy}$ using single-date, scaled-up MODIS observations; (2) to apply the $FAPAR_{chl}$ and $FAPAR_{canopy}$ algorithms to MODIS data acquired for 2001-2005 over this aspen flux site in Saskatchewan; (3) to link our estimates of MODIS $FAPAR_{chl}$ and $FAPAR_{canopy}$ to the tower-based observations of PAR and GEP so as to derive LUE on both a unit cholorophyll area basis (LUE_{chl}, Eq.3 above) and for the whole canopy (LUE_{canopy}, Eq.4 above); and (4) to compare our LUE_{chl}, LUE_{canopy} and tower-based LUE estimates (i.e., LUE_{tower}) to see if the LUE_{chl} could provide a more physiologically realistic input to land surface process models. For this latter objective, we test the hypotheses that: (i) $LUE_{canopy} = LUE_{chl}$; (ii) $LUE_{chl} = LUE_{tower}$; and (iii) $LUE_{canopy} = LUE_{tower}$.

2. Data and site descriptions

2.1 Southern Old Aspen

The Southern Old Aspen forest (SOA) was established in 1919 after a forest fire in Prince Albert National Park at the southern edge of the Canadian boreal forest (Barr *et al.* 2007). The eddy flux tower site (53.7°N, 106.2°W, 600 m elevation) is located ~50 km northwest of Prince Albert, Saskatchewan. SOA originated as part of the BOReal Ecosystem Atmosphere Study (BOREAS), and has continued operations under the Boreal Ecosystem Research and Monitoring Sites (BERMS) project and the Canadian Carbon Program, formerly the Fluxnet-Canada Research Network (FCRN). The vegetation around the tower site is primarily deciduous forest dominated 90% by aspen (*Populus tremuloides* Michx.) with 10% balsam poplar (*Populus balsamifera* L.) and a dense understory approximately 2 m tall of hazelnut (*Corylus cornuta* Marsh) interspersed with green alder (*Alnus crispa* Pursch). The aspen stand extends for at least 3 km in all directions from the tower. The soil is mainly an orthic grey luvisol with a ~9 cm surface organic layer. The terrain is basically level. Mid-growing season leaf area index (LAI) under the tower varied from ~3.5 to 5.5. The climate is warm in summer (av. 17.5°C in July) and cold in winter (av. -19.1°C in January). Average annual precipitation was 412 mm during 2001-2005, whereas the long-term 1951-1980 average annual precipitation was higher at 484 mm (Griffis *et al.* 2003). A detailed analysis of the inter-annual variability of climatic factors at this site is presented in Barr *et al.* (2007).

2.2 GEP Data

GEP at SOA was estimated as the sum of Net Ecosystem Production (NEP) and ecosystem respiration. Respiration was modeled from night time and cold season NEP using soil

temperature. Details on CO_2 flux measurement methodology and obtaining estimates of GEP including gap filling can be found in Krishnan *et al.* (2006) and Barr *et al.* (2007).

2.3 Daily MODIS data

Four MODIS daily products (v004) were used in this study: [1] surface reflectance (MOD09GHK and MYD09GHK); [2] observation viewing and illumination geometry (MODMGGAD and MYDMGGAD); [3] observation pointer information (MODPTHKM and MYDPTHKM); and [4] reflectance data quality descriptors (MOD09GST and MYD09GST). The MODIS imagery is nominally acquired with 500 m x 500 m spatial resolution at nadir, and >500 m spatial resolution for off-nadir views. The MODIS daily land surface reflectance product provides seven (of 36) spectral bands: red (620–670 nm, band 1), blue (459–479 nm, band 3), green (545–565 nm, band 4), near infrared (NIR_1, 841–875 nm, band 2; NIR_2, 1230–1250 nm, band 5), and short-wave infrared ($SWIR_1$, 1628–1652 nm, band 6; $SWIR_2$, 2105–2155 nm, band 7).

The MODIS daily observation viewing geometry product provides viewing and illumination geometry information (view zenith angle, VZA; view azimuth angle; sun zenith angle; and sun azimuth angle) at a nominal 1-km scale. The MODIS daily observation pointer product provides a reference, at a nominal 500 m scale, linking observations that intersect each pixel in the daily surface reflectance product to those given in the daily observation viewing geometry product. The MODIS daily reflectance data quality product provides summary quality information about MODIS daily surface reflectance conditions, including clouds, cloud shadow, land and water designations, aerosols, fire, snow, ice and bidirectional reflectance distribution function (BRDF) corrections, etc. All the MODIS data products are freely available at USGS

Earth Observing System Data Gateway (http://edcimswww.cr.usgs.gov/pub/imswelcome/), and are delivered to users in a tile fashion, where each tile covers an area of 10° (latitude) by 10° (longitude). The software developed by the MODIS land team (MODLAND Tile Calculator http://modland.nascom.nasa.gov/cgi-bin/developer/tilemap.cgi) was utilized to determine the location of the SOA tower site in the MODIS products, including tile, row and column numbers.

3. Methods

3.1 Spatial integration of MODIS data

A possible source of discrepancy between tower-based photosynthesis and the MODIS standard GPP is the way the MODIS reflectance products are used to calculate $FAPAR_{canopy}$ and the MODIS standard GPP (Justice *et al.* 1998; Wolfe *et al.* 1998). This occurs because the areal coverage of the MODIS products used in the GPP calculations are not constant over the growing season and may not match the footprint of the flux tower site. The MODIS observations made at multiple times over a target actually cover somewhat different ground areas due to shifts in the ground track of the satellite, but are gridded into single, fixed grid cells. Footprints for off-nadir observations are increasingly larger and oblong in shape as VZAs increase. For example, areas associated with ground targets for imagery acquired with VZAs greater than 65^{o} are at least nine times larger than those viewed by nadir observations (Wolfe *et al.* 1998). Consequently, both the standard MODIS $FAPAR_{canopy}$ and GPP products represent somewhat different, though overlapping or adjacent, areas when viewed frequently over time with different geometries.

For the current analysis, we developed a method to scale-up the MODIS land band observations to 2500 m x 2500 m regions. We assumed that the scaled-up satellite 2500 m data and tower flux-based data should follow a similar pattern, although they are not necessarily

identical. This is a reasonable assumption since the flux footprint for the site described in the current study extends for at least three km in all directions from the flux tower.

We acquired daily MODIS data (tile H11V04) for 2001-2005. An example is given (Figure 1) for MODIS daily NIR_1 reflectances across the 5x5 grid area (where each grid cell is nominally 500 m) for nadir data on day of year (DOY) 224 in 2001. The MODIS relative reflectance data quality descriptor indicates that the reflectances were of high quality.

We used 5x5 scaled up MODIS observations to produce similar ground sectors within the 2.5 km x 2.5 km block area of the aspen forest (as in Fig. 1). A time series for the 5x5 block was created from MODIS daily data using the following criteria: (i) only observations that fell within the block were selected; (ii) an observation was excluded from consideration if the reflectance quality product indicated any quality problem; (iii) observations were averaged only if their geometries for view and illumination angles differed by less than five degrees; (iv) observations from different swaths were not mixed; and (v) the inclusion of at least 18 of the 25 grid cells were required to produce a scaled-up average observation for use in the subsequent analysis (Table 1).

The NDVI time series (Tucker 1979, Eq. 5 below) over five years (2001-2005) were used to determine average core growing season length where:

$$NDVI = \frac{\rho_{NIR_1} - \rho_{red}}{\rho_{NIR_1} + \rho_{red}}. \qquad (5)$$

Other remote sensing indices were explored, e.g. the enhanced vegetation index (EVI; Huete *et al.* 1994) and the land surface water index (LSWI, Xiao *et al.* 2005), but NDVI gave more coherent seasonal results (data not shown). Degree 6 polynomials were used to fit average seasonal curves to the five-year data collections for the MODIS NDVI and the mid-day tower

GEP, respectively. Derivative analyses were applied to the fitted curves. We used the first, second, and third derivatives to identify transition points in continuous data curves (Vina *et al.* 2004) to retrieve the DOY in the five-year collections when seasonal changes occurred. We defined the beginning date of the growing season as the date when the second derivative reached its first local extreme value during the spring green-up period. We defined the end date for the growing season as that date when either the first or third derivatives attained a local extreme value at the end of summer (DOY > 255 at this site), initiating autumn senescence. Based on these analyses, we used NDVI for examining LUE and FAPAR dynamics for the photosynthetically active period, defined as occurring between DOY 152-259. We also defined the earlier and later dates for a second category representing periods of lower physiological activity (DOY between 121 and 151 and DOY between 260 and 287).

3.2 Estimating vegetation canopy characteristics

3.2.1 Description of the PROSAIL-2 model

The canopy-leaf-stem-background coupled radiative transfer model, PROSAIL-2, is an updated version of the model used in earlier studies (Zhang *et al.* 2005, 2006). PROSAIL-2 resulted from the combination of the PROSPECT model used to describe leaf characteristics in the canopy model, and the radiative transfer model, SAIL2. In the current version of SAIL2, we revised the expression for background and stem characteristics. Equations 5 & 6 in Zhang *et al.* (2006) were used to simulate soil and stem reflectance. In the present study, we used *in situ* measurements from the Oak Ridge National Laboratory website: (http://www.daac.ornl.gov/BOREAS/boreas_home_page.html) to provide the "search ranges" for background (referred to as "back") and stem spectral reflectance (referred to as "stem").

$$\rho_{back}(\lambda) = \rho_{back,\min}(\lambda) + BACK_A \bullet (\rho_{back,\max}(\lambda) - \rho_{back,\min}(\lambda)) \quad (6)$$

$$\rho_{stem}(\lambda) = \rho_{stem,\min}(\lambda) + STEM_A \bullet (\rho_{stem,\max}(\lambda) - \rho_{stem,\min}(\lambda)), \quad (7)$$

where λ is the spectral wavelength, ρ is reflectance, $BACK_A$ and $STEM_A$ are variables describing reflectance values for background and stem. We used the maximum and minimum reflectance values of background and stem as their upper and lower value limits. The fourteen free variables used in the PROSAIL-2 for this study are summarized in Table 2. Five variables were used to describe leaf characteristics: a leaf internal structure variable (N), leaf total photosynthetic pigment content (C_{ab}), leaf dry matter content (C_m), leaf water thickness (C_w), and leaf brown pigment content (C_{brown}). The top of canopy reflectance was composed of leaf, stem and background contributions. Stem fraction (SFRAC) and cover fraction (CF) were used to decompose leaf, stem and background components. Refer to Zhang *et al.* (2005, 2006) for more details on PROSAIL-2.

3.2.2 Description of the $FAPAR_{chl}$ and $FAPAR_{canopy}$ algorithm

The variables in Tab. 2 have to be estimated to calculate $FAPAR_{chl}$ and $FAPAR_{canopy}$ using PROSAIL-2. The Metropolis algorithm, a Markov Chain Monte Carlo (MCMC) method, was adopted to find solutions expressed as posterior distributions of the variables. The posterior distributions of the variables are the product of their prior distributions and the likelihood calculated with a Bayesian analysis (http://en.wikipedia.org/wiki/Posterior_probability). The prior distributions of the input variables were assumed to be uniform (http://en.wikipedia.org/wiki/Uniform_distribution_(continuous)). Each MODIS reflectance observation [ρ_{obs}] for the seven land bands (red, NIR_1, blue, green, NIR_2, $SWIR_1$ and $SWIR_2$), and associated VZA [θ_v, in degrees], relative view azimuth angle [ϕ, in degrees], and solar zenith angle [θ_s, in degrees]

contains some noise, although small differences in angles may be ignored. We treat each SOA reflectance observation as a sample of the following distribution:

$$\rho \sim \{\rho_{obs}(\lambda, \theta_v(1+3\mathrm{N}(0,1)), \theta_s(1+3\mathrm{N}(0,1)), \phi(1+3\mathrm{N}(0,1)))\} \cdot (1+0.05\mathrm{N}(0,1)) \quad (8)$$

where N(0,1) is the normal distribution with a mean of zero and SD = 1.

We may use as many samples from the distribution (from equation 8) as we desire. For five of the spectral bands (red, green, NIR_1, NIR_2 and $SWIR_1$), we calculated the log-likelihood [using equations 1& 2 from Zhang *et al.* 2005] and then performed an acceptance test [using equation 3 from Zhang *et al.* 2005]. A new randomly generated "proposed" value was accepted only if it passed acceptance tests conducted on all five bands. The same adaptive algorithm [using equation 4 from Zhang *et al.* 2005] was used to accelerate the speed of convergence of the MCMC algorithm. With the posterior distributions of the variables (Tab. 2) now calculated, we forward-simulated the fractions of APAR for canopy, leaf, and photosynthetic pigments (Zhang *et al.* 2005, 2006) for each MODIS 5x5 scaled-up observation that met our quality rules during the five-year period, using the PROSAIL-2 model. The product of LAI, CF, and leaf photosynthetic pigment ($\mu g/cm^2$) describes the average photosynthetic pigment content for each 5x5 MODIS aspen forest observation. Similarly, the product of LAI, CF and leaf water content (cm) describes the average water content of vegetation and, the product of LAI, CF and leaf dry matter (g/cm^2) provides the average dry matter content of vegetation in each MODIS observation.

3.2.3 *Calculation of $APAR_{chl}$, $APAR_{canopy}$, LUE_{chl}, LUE_{canopy} and LUE_{tower}*

The PAR absorbed by the whole SOA canopy ($APAR_{canopy}$) was determined as the product of PAR and the median value of the MODIS-derived $FAPAR_{canopy}$ distribution (see section above). Likewise, $APAR_{chl}$ for only the photosynthetic pigments of the foliage component was determined as the product of PAR and the median value of the MODIS-derived $FAPAR_{chl}$ distribution. For these calculations, we used the GEP and average incident canopy photosynthetic photon flux density (PPFD) measured with Li-190SA PAR sensors (Licor Inc., Lincoln, NE) over the SOA tower site at 90-minute intervals centered on the satellite overpass time. LUE for the foliage component of the forest at SOA (LUE_{chl}, Eq.3) was computed as the ratio of GEP to $APAR_{chl}$. LUE for the whole SOA forest canopy (LUE_{canopy}, Eq.4) was computed as the ratio of GEP to $APAR_{canopy}$. The LUE_{tower} (Eq. 2 above) data used in this paper are cited from Krishnan *et al.* (2006) where they defined LUE_{tower} as the ratio $GEP_{tower}/APAR_{tower}$ where $APAR_{tower}$ was estimated using Eq. (1) in Barr *et al.* (2007) that was based on measured downwelling and upwelling PAR, overstory and understory clumping indices, measured stem area indices, and the estimated daily LAI. Therefore, LUE_{canopy} and LUE_{chl} use MODIS-derived FAPARs whereas LUE_{tower} derives its FAPAR equivalent from site-based radiometer and structural measurements. The GEP and PAR variables, on the other hand, are the same for the three LUE calculations.

The REGRESS function in MATLAB was used to statistically analyze regression relationships between: (i) GEP and $APAR_{chl}$; (ii) GEP and $APAR_{canopy}$; (iii) annual average LUE_{chl};and annual average LUE_{canopy} over the five-year core growing season period; and (iv) annual average LUE_{tower} and annual average LUE_{chl}. We also used the student t-test function in MATLAB to test if the slope between GEP and $APAR_{chl}$ and the slope between GEP and

$APAR_{canopy}$ were significantly different. The same t-test function was also applied to test if the annual average LUE_{chl}, LUE_{canopy} and LUE_{tower} time series over the entire five-year period were significantly different.

3.2.4 Controls on inter-annual LUE_{chl} and LUE_{canopy}

To determine the controls on the inter-annual variation of LUE, we analyzed the relationship between LUE_{chl}, LUE_{canopy}, soil water content (SWC), and precipitation as well as the three factors that determine canopy chlorophyll concentration, i.e., average leaf chlorophyll concentration, leaf area index (LAI), and cover fraction (CF). Soil water content was measured with eight time domain reflectometry (TDR) probes (Moisture Point type B, Gabel Corp., Victoria, Canada) placed at 10 m intervals with measurements at depths of 0-15, 15-30, 30-60, 60-90, and 90-120 cm, although SWC values were used only for the 0-30 cm zone because this is where 90% of the roots are found (Barr *et al.* 2007). Rain precipitation was measured with a Geonor T200 accumulation rain gauge (Geonor Inc, Milford, PA) supplemented by a CS700 tipping bucket rain gauge (Campbell Scientific Inc, Edmonton, AB). The half-hourly precipitation measurements at the SOA tower site in 2001-2005 were summed into monthly rain precipitation totals, from which annual values were 235 mm, 285.8 mm, 261 mm, 667 mm and 614 mm for 2001 - 2005, respectively.

4. Results

4.1 PROSAIL-2 Derived Canopy Variables including $APAR_{chl}$ and $APAR_{canopy}$

The posterior distributions of SOA canopy variables from the PROSAIL-2 model display seasonal variation, as shown for nine of the seventeen MODIS daily 5x5 observations in 2005

(Table 3). The other observations had similar distributions as those shown in Tab. 3 so they are not presented. Several canopy variables are shown: LAI, CF, total photosynthetic pigment content, water content, dry matter content, $FAPAR_{canopy}$, and $FAPAR_{chl}$. Differences in total chlorophyll concentration were related to changes in all three of the factors used in its calculation, i.e., average leaf chlorophyll concentration, LAI, and CF. The considerably higher $FAPAR_{canopy}$ (0.47 – 0.87), as compared to $FAPAR_{chl}$ (0.03 – 0.70), results from PAR absorption primarily by non-photosynthetic canopy components. The average $APAR_{chl}$ at SOA over the five-year period was roughly 65% of $APAR_{canopy}$ (slope of the all-data relationship in Fig. 2). We also found that the average ratios for $APAR_{chl}$: $APAR_{canopy}$ were different between the core growing season, DOY 152 – 259 (♦, slope = 0.71); and the combined early and late periods of the season, DOY <152 and DOY>259 (Δ, slope = 0.34) (Fig. 2). The correlation between $APAR_{chl}$ and $APAR_{canopy}$ showed the highest correlation (r = 0.87) during the core growing season, DOY 152-259 (Fig. 2).

4.2 *LUE_{chl} and LUE_{canopy} Over the Five-Year Period*

Average values for LUE_{canopy} and LUE_{chl} over the five-year period (2001-2005) were 0.0155 and 0.0241 μmol C μmol^{-1} PPFD, respectively, as determined from the slopes of the GEP:APAR relationships (Figure 3 for $APAR_{canopy}$; Figure 4 for $APAR_{chl}$, $p<0.0001$). For the entire study period (DOY ranging from 121 to 287), there was a stronger correlation between GEP and APARchl, (Fig. 4, $r^2 = 0.78$) compared $GEP:APAR_{canopy}$ (Fig. 3, $r^2 = 0.33$). The 95% confidence intervals for the five-year average LUE_{canopy} and LUE_{chl} did not overlap, i.e., they ranged from 0.0141 to 0.0169 and from 0.0229 to 0.0253, respectively.

For the core growing season only (DOY 152 – 259), the five-year average values of LUE_{canopy} and LUE_{chl} were 0.0173 and 0.0243 μmol C μmol^{-1} PPFD, respectively (Figure 3 for $APAR_{canopy}$; Figure 4 for $APAR_{chl}$, $p<0.0006$). Once again, the 95% confidence intervals for the five-year average LUE_{canopy} and LUE_{chl} did not overlap, i.e., they ranged from 0.0163 to 0.0183 and from 0.0230 to 0.0256, respectively.

$APAR_{chl}$ and LUE_{chl} captured more seasonal variation than their whole canopy counterparts ($APAR_{canopy}$, LUE_{canopy}) (Figs. 3 and 4). For example, during the early and late growing season, average LUE_{chl} over five years was 0.0208 μmol C μmol^{-1} PPFD which was lower than the core growing season value of 0.0243 μmol C μmol^{-1} PPFD (Fig. 4).

4.3 Inter-Annual Variability in LUE

There were also inter-annual variations for $APAR_{chl}$ and $APAR_{canopy}$ (mean ± SE, the standard error) with consistently and significantly lower values for $APAR_{chl}$ compared to $APAR_{canopy}$ during the core growing season (Figure 5) ($p<0.005$). Consequently, LUE_{chl} was consistently and significantly higher than LUE_{canopy} (Figure 6) ($p<0.005$) and LUE_{chl} in 2004-2005 was higher than for the three earlier years during the growing season. The effect of the 2003 drought was apparent, such that the average LUE_{chl} and LUE_{canopy} in 2004 were much higher than in 2003. The annual means of core growing season LUE_{chl} (μmol C μmol^{-1} PPFD) (± SE) were: 0.0242 ± 0.0012 (2001), 0.0245 ± 0.0015 (2002); 0.0225 ± 0.0018 (2003); 0.0310 ± 0.0022 (2004); and 0.0267 ± 0.0019 (2005) (Tab. 4). The maximum LUE (ε_{max}) value for broadleaf deciduous forests set by the biome look-up table of the MODIS photosynthesis model is 0.0203 μmol C μmol^{-1} PPFD (Heinsch et al., 2003). Four of the five annual LUE_{canopy} values

that we calculated were lower than ε_{max}. However, the 2004 LUE_{canopy} was much higher than the MODIS ε_{max} value (Fig. 6).

Average LAI, CF, canopy chlorophyll concentration, $FAPAR_{canopy}$, $FAPAR_{chl}$, LUE_{canopy} and LUE_{chl} during core growing season ($152 \leq DOY \leq 259$) for each individual year are shown in Table 4. Inter-annual variations of canopy chlorophyll concentration were influenced by all the three factors ($r^2 = 0.91$ for leaf chlorophyll concentration; $r^2 = 0.32$ for LAI; and $r^2 = 0.49$ for CF). Average annual canopy chlorophyll concentrations were correlated with both $FAPAR_{chl}$ ($r^2 = 0.81$) and $APAR_{chl}$ ($r^2 = 0.63$).

4.4. Comparisons with LUE_{tower}

Whereas LUE_{canopy} differed significantly from LUE_{tower} for each of the five years ($p \leq 0.001$), LUE_{chl} was essentially the same as LUE_{tower} ($p \geq 0.47$, Figure 6).

5. Discussion

LUE_{chl} captured more seasonal (Tab. 3) and inter-annual variation than LUE_{canopy} and provided an improved overall relationship to GEP (Figs. 3 and 4). Krishnan *et al.* (2006) reported that the annual average LUE_{tower} at the SOA tower for 2001-2005 was 0.0229 – 0.0302 μmol C μmol^{-1} PPFD. Their *in situ* average LUE_{tower} estimate matched well with our average MODIS-derived LUE_{chl} (0.0229 – 0.0302 vs. 0.0225 – 0.0310 μmol C μmol^{-1} PPFD from Fig. 4) but not with the MODIS-derived LUE_{canopy} over five growing seasons. Furthermore, the *in situ* tower-based LUE_{tower} and the MODIS-derived LUE_{chl} were also similar in each of the five years, exhibiting their highest values in 2004-2005 (Fig. 6).

The annual LUE_{canopy} values substantially underestimated the tower-based estimates (Krishnan *et al.* 2006) (Fig. 6). It is interesting to note that the five-year average LUE_{canopy} for the mid-growing season period was higher than LUE_{canopy} for the early and late season periods (Fig. 3). In comparison, the five-year average LUE_{chl} for all data was consistent with LUE_{chl} for the mid-growing season period, and also close to LUE_{chl} for the early and late season periods (Fig. 4). Additionally, the maximum LUE value (ε_{max}) from the MODIS biome look-up table for broadleaf deciduous forests (Heinsch *et al.* 2003) tended to be significantly lower than both LUE_{chl} and LUE_{tower} (Fig. 6). This study has demonstrated that (1) LUE_{chl} values are more comparable to ground-based observations of LUE_{tower} than LUE_{canopy}; (2) $APAR_{chl}$ values are more comparable to ground-based observations of $APAR_{tower}$ when the sky is clear than $APAR_{canopy}$; (3) $FAPAR_{chl}$ values derived from MODIS observations are more realistic and useful for estimating of $APAR_{tower}$ when the sky is clear than $FAPAR_{canopy}$ values. The conclusions are supported by measurements and simulations of photosynthetic vs. non-photosynthetic vegetation by Chen *et al.* (2006) at other flux sites in the region. Consequently, we accept the hypothesis that $LUE_{chl} = LUE_{tower}$, whereas we reject the other two hypotheses that $LUE_{canopy} = LUE_{chl}$ or that $LUE_{canopy} = LUE_{tower}$.

A prolonged three-year drought began in late summer of 2001 and the most severe conditions occurred in 2003 (Barr *et al.* 2007), which also produced the lowest LUE_{chl} (Fig. 6). There were eleven consecutive months prior to August 2003 when precipitation was <50 mm per month. The water table depth decreased from 3 m in 2001 to 4 m in 2003 (Barr *et al.* 2007). Low precipitation in 2001 through 2003 caused soil water content in the shallow layer (0-0.15 m) to begin to drop in August 2001 and it kept dropping through 2002 and 2003. The lowest soil water content occurred in 2003 and was one-third lower than the pre-drought mean value and was close

to the permanent wilting point. Surface conductance declined during the drought years and reached its lowest value in 2003 (Krishnan *et al.* 2006). Figure 7 compares the average LUE_{chl} and LUE_{canopy} during DOY 152-259 of each year (2001 - 2005) with the cumulative rain precipitation during that time period. This analysis suggests that the cumulative precipitation during 2001-2005 may have had a significant influence on LUE. Increased rain precipitation in 2004 and 2005 recharged the soil and increased LUE and our MODIS-based LUE_{chl} estimates were sensitive to this phenomenon.

$FAPAR_{chl}$ and LUE_{chl} are more physiologically realistic ways of quantifying the PAR absorbed and used for photosynthesis. These are integrative measures that inherently account for some of the impacts of mid- to long-term stresses since they also reflect changes in leaf area and cover fraction. For example, inter-annual variability of total canopy chlorophyll concentration was influenced by changes in average leaf chlorophyll concentration, LAI and CF (Table 4). The 2003 drought lowered all three of these factors at our study area relative to 2001 and 2002. Thus, chlorophyll-based measures of APAR and LUE have the potential to more directly account for environmental limitations and thus reduce the impact of the uncertainty in estimating temperature, vapor pressure deficit, and soil moisture for specific pixels. Waring *et al.* (1995) found a strong correlation between upper canopy leaf chlorophyll concentration of the major hardwood species and maximum light use efficiency at the primarily deciduous Harvard Forest flux site. Their finding supports the idea of a direct link between pigment concentration and LUE_{tower} for deciduous forests. Ollinger *et al.* (2008) and Kergoat et al. (2008) showed a significant positive relationship between whole canopy nitrogen concentration and canopy maximum LUE but the relationship between canopy nitrogen and chlorophyll was not described and they did not examine inter-annual or seasonal variability at any of their sites. Their results

lead us to believe that an inter-site analysis based on $APAR_{chl}$ and LUE_{chl} using our methodology would yield even stronger relationships.

Chlorophyll-based measures of APAR and LUE, however, will not account for limitations due to short-term environmental extremes so modulation of light use efficiency by environmental stresses will still need to be considered. Furthermore, photosynthesis of evergreen conifer forests are less sensitive to changes in chlorophyll than are broadleaf forests as evidenced by the continuous green color of conifer forests even during the coldest periods of winter. As well, forests that have attained maximum height are subject to significant hydraulic and stomatal limitations (Ryan *et al.* 2004, 1997) that may or may not be reflected in their total canopy chlorophyll concentration. Brodribb and Feild (2000) demonstrated a highly significant correlation between hydraulic conductivity, maximum photosynthetic capacity, and quantum yield 23 rain forest species.

To our knowledge, this study represents the first time that LUE_{chl} has been estimated by linking tower flux data, a biophysical radiative transfer model, and satellite spectral observations. Our predicted values for LUE_{chl} agree well with *in situ* data in respect to both amplitude and seasonal phase; and our modeled LUE_{chl} successfully described the actual dynamics captured by tower fluxes. We believe that it could be useful to couple this type of $FAPAR_{chl}$ approach into regional/global carbon cycle models, land surface process models and general circulation models.

This paper has demonstrated some of the possible benefits of using $FAPAR_{chl}$ as an operational data product for carbon cycle modeling. The hyperspectral satellite sensors that are in orbit (e.g., EO-1/Hyperion) or currently under development (e.g., HyspIRI) could help us obtain even more robust estimates of $FAPAR_{chl}$ due to the greater sensitivity of these sensors to pigment concentrations and other biochemical properties of foliage (Coops e*t al.* 2002). A

narrower field of view could also be helpful for resolving chlorophyll dynamics at scales more representative (e.g., <100 m) of the spatial structure typical of most forest stands.

6. Acknowledgments

This project was supported by the NASA Carbon Cycle Science Program (Dr. Diane Wickland, Program Manager) under the auspices of the North American Carbon Program. Support was provided to the FCRN and BERMS programs through several Canadian funding sources (Environment Canada, the Canadian Forest Service, NSERC, CFCAS, BIOCAP, Action Plan 2000 and PERD).

7. References

Barr, A.G., Black, T.A., Hogg, E.H., Griffis, T.J., Morgenstern, K., Kljun, N., Theede, A., & Nesic, Z. (2007). Climatic controls on the carbon and water balances of a boreal aspen forest, 1994-2003. *Global Change Biology, 13*, 561-576.

Brodribb, T.J. & Feild, T.S. (2000). Stem hydraulic supply is linked to leaf photosynthetic capacity: evidence from New Caledonian and Tasmanian rainforests. *Plant, Cell and Environment* 23, 1381-1388

Coops, N.C., Smith, M.-L., Martin, M.E., Ollinger, S.V., & Held, A. (2002). Predicting eucalypt biochemistry from HYPERION and HYMAP imagery. *IGARSS'02, 2*, 790 - 792

Gower, S.T., Kucharik, C.J., & Norman, J.M. (1999). Direct and indirect estimation of leaf area index, fAPAR and net primary production of terrestrial ecosystems. *Remote Sensing of Environment, 70*, 29-51

Griffis, T.J., Black, T.A., Morgenstern, K., Barr, A.G., Nesic, Z., Drewitt, G.B., Gaumont-Guay, D., & McCaughey, J.H. (2003). Ecophysiological controls on the carbon balances of three southern boreal forests. *Agricultural and Forest Meteorology, 117*, 53-71

Heinsch, F.A., M. Reeves, P. Votava, S. Kang, C. Milesi, M. Zhao, J. Glassy, W.M. Jolly, R. Loehman, C.F. Bowker, J. Kimball, R. Nemani, S.W. Running. (2003). User's Guide: GPP and NPP (MOD17A2/A3) Products. NASA MODIS Land Algorithm. Version 2.0. NASA Algorithm Theoretical Basis Document (ATBD).

Huete, A., Justice, C., & Liu, H. (1994). Development of Vegetation and Soil Indexes for Modis-Eos. *Remote Sensing of Environment, 49*, 224-234

Justice, C.O., Vermote, E., Townshend, J.R.G., Defries, R., Roy, D.P., Hall, D.K., Salomonson, V.V., Privette, J.L., Riggs, G., Strahler, A., Lucht, W., Myneni, R.B., Knyazikhin, Y., Running, S.W., Nemani, R.R., Wan, Z.M., Huete, A.R., van Leeuwen, W., Wolfe, R.E., Giglio, L., Muller, J.P., Lewis, P., & Barnsley, M.J. (1998). The Moderate Resolution Imaging Spectroradiometer (MODIS): Land remote sensing for global change research. *IEEE Transactions on Geoscience and Remote Sensing, 36*, 1228-1249

Kergoat, L., Lafont, S., Arneth, A., Le Dantec, V., & Saugier, B. (2008). Nitrogen controls plant canopy light-use efficiency in temperate and boreal ecosystems. *Journal of Geophysical Research*, 113, G04017, doi:10.1029/2007JG000676.

Krishnan, P., Black, T.A., Grant, N.J., Barr, A.G., Hogg, E.H., Jassal, R.S., & Morgenstern, K. (2006). Impact of changing soil moisture distribution on net ecosystem productivity of a boreal aspen forest during and following drought. *Agricultural and Forest Meteorology, 139*, 208-233

Landsberg, J.J., & Waring, R.H. (1997). A generalized model of forest productivity using simplified concepts of radiation-use efficiency, carbon balance and partitioning. *Forest Ecology and Management, 95*, 209–228

Law, B.E., Waring, R.H., Anthoni, P.M., & Aber, J.D. (2000). Measurements of gross and net ecosystem productivity and water vapour exchange of a Pinus ponderosa ecosystem, and an evaluation of two generalized models. *Global Change Biology, 6*, 155-168

Medlyn, B.E. (1998). Physiological basis of the light use efficiency model. *Tree Physiology, 18*, 167-176

Mohr, H., Schopfer, P., Lawlor, G., & Lawlor, D.W. (Eds.) (1995). *Plant Physiology*: Springer

Monteith, J.L. (1972). Solar-Radiation and productivity in tropical ecosystems. *Journal of Applied Ecology, 9*, 747-766

Monteith, J.L. (1977). Climate and efficiency of crop production in Britain. *Philosophical Transaction of the Royal Society of London B: Biological Sciences, 281*, 271-294

Ollinger, S.V., Richardson, A.D., Martin, M.E., Hollinger, D.Y., Frolking, S.E., Reich, P.B., Plourde, L.C., Katul, G.G., Munger, J.W., Oren, R.O., Smith, M.-L., Paw U, K.T., Bolstad, P.V., Cook, B.D., Day, M.C., Martin, T.A., Monson, R.K., & Schmid, H.P. (2008). Canopy nitrogen, carbon assimilation, and albedo in temperate and boreal forests: Functional relations and potential climate feedbacks. *Proceedings, National Academy of Sciences,* 105, 19336-19341.

Prince, S.D., Goetz, S.J., & Goward, S.N. (1995). Monitoring Primary Production from Earth Observing Satellites. *Water Air and Soil Pollution, 82*, 509-522

Prince, S.D., & Goward, S.N. (1995). Global primary production: A remote sensing approach. *Journal of Biogeography, 22*, 815-835

Prince, S.D., & Goward, S.N. (1996). Evaluation of the NOAA/NASA Pathfinder AVHRR Land Data Set for global primary production modelling. *International Journal of Remote Sensing, 17*, 217-221

Prince, S.D., Goward, S.N., Goetz, S., & Czajkowski, K. (2000). Interannual Atmosphere-Biosphere Variation: Implications for observation and modeling. *Journal of Geophysical Research-Atmospheres, 105*, 20055-20063

Ruimy, A., Dedieu, G., & Saugier, B. (1996a). TURC: A diagnostic model of continental gross primary productivity and net primary productivity. *Global Biogeochemical Cycles, 10*, 269-285

Ruimy, A., Kergoat, L., Field, C.B., & Saugier, B. (1996b). The use of CO2 flux measurements in models of the global terrestrial carbon budget. *Global Change Biology, 2*, 287-296

Ruimy, A., Saugier, B., & Dedieu, G. (1994). Methodology for estimation of terrestrial net primary production from remotely sensed data. *Journal of Geophysical Research - Atmospheres, 99*, 5263-5283

Running, S., Nemani, R., Heinsch, F., Zhao, M., Reeves, M., & Hashimoto, H. (2004). A continuous satellite-derived measure of global terrestrial primary production. *BioScience, 54*, 547-560

Running, S.W., Baldocchi, D.D., Turner, D.P., Gower, S.T., Bakwin, P.S., & Hibbard, K.A. (1999a). A global terrestrial monitoring network integrating tower fluxes, flask sampling, ecosystem modeling and EOS satellite data. *Remote Sensing of Environment, 70*, 108-127

Running, S.W., Justice, C.O., Salomonson, V., Hall, D., Barker, J., Kaufmann, Y.J., Strahler, A.H., Huete, A.R., Muller, J.P., Vanderbilt, V., Wan, Z.M., Teillet, P., & Carneggie, D.

(1994). Terrestrial Remote-Sensing Science and Algorithms Planned for Eos Modis. *International Journal of Remote Sensing, 15*, 3587-3620

Running, S.W., Nemani, R., Glassy, J.M., & Thornton, P.E. (1999b). MODIS daily photosynthesis (PSN) and annual net primary production (NPP) product (MOD17), Algorithm Theoretical Basis Document, Version 3.0

Running, S.W., Thornton, P.E., Nemani, R., & Glassy, J.M. (2000). Global terrestrial gross and net primary productivity from the Earth Observing System. In O.E. Sala, R.B. Jackson, H.A. Mooney & R.W. Howarth (Eds.), *Methods in Ecosystem Science* (pp. 44-57). New York: Springer Verlag

Ryan M.G., Binkley D., Fownes J.H. (1997) Age-related decline in forest productivity: pattern and process. Advances in Ecological Research, 27, 213–262.

Ryan M.G., Binkley D., Fownes J.H., Giardina C.P., Senock, R.S. (2004). An experimental test of the causes of forest growth decline with stand age. Ecological Monographs, 74, 393–414.

Sellers, P.J., Los, S.O., Tucker, C.J., Justice, C.O., Dazlich, D.A., Collatz, G.J., & Randall, D.A. (1996a). A revised land surface parameterization (SiB2) for atmospheric GCMs .2. The generation of global fields of terrestrial biophysical parameters from satellite data. *Journal of Climate, 9*, 706-737

Sellers, P.J., Randall, D.A., Collatz, G.J., Berry, J.A., Field, C.B., Dazlich, D.A., Zhang, C., Collelo, G.D., & Bounoua, L. (1996b). A revised land surface parameterization (SiB2) for atmospheric GCMs .1. Model formulation. *Journal of Climate, 9*, 676-705

Tucker, C.J. (1979). Red and Photographic Infrared Linear Combinations for Monitoring Vegetation. *Remote Sensing of Environment, 8*, 127-150

Turner, D.P., Ollinger, S., Smith, M.L., Krankina, O., & Gregory, M. (2004). Scaling net primary production to a MODIS footprint in support of Earth observing system product validation. *International Journal of Remote Sensing, 25*, 1961-1979

Turner, D.P., Ritts, W.D., Cohen, W.B., Gower, S.T., Zhao, M.S., Running, S.W., Wofsy, S.C., Urbanski, S., Dunn, A.L., & Munger, J.W. (2003). Scaling Gross Primary Production (GPP) over boreal and deciduous forest landscapes in support of MODIS GPP product validation. *Remote Sensing of Environment, 88*, 256-270

Turner, D.P., Ritts, W.D., Zhao, M., Kurc, S.A., Dunn, A.L., Wofsy, S., Small, E., & Running, S.W. (2006). Assessing interannual variation in MODIS-based estimates of gross primary production. *Ieee Computational Science & Engineering, 44*, 1899-1907

Vina, A., A. Gitelson, D. Rundquist, G. Keydan, B. Leavitt, and J. Schepers (2004). Monitoring Maize (*Zea mays* L.) Phenology with Remote Sensing. *Agronomy Journal* 96:1139-1147.

Waring, R.H., Law, B.E., Goulden, M.L., Bassow, S.L., McCreight, R.W., Wofsy, S.C., Bazzaz, F.A. (1995). Scaling gross ecosystem production at Harvard Forest with remote sensing: a comparison of estimates from a constrained quantum-use efficiency model and eddy correlation. *Plant, Cell, Environment 18*, 1201-1213.

Wolfe, R., Roy, D., & Vermote, E. (1998). The MODIS land data storage, gridding and compositing methodology: Level 2 Grid. *IEEE Transactions on Geosciences and Remote Sensing, 36*, 1324-1338

Xiao, X.M., Zhang, Q.Y., Hollinger, D., Aber, J., & Moore, B. (2005). Modeling gross primary production of an evergreen needleleaf forest using modis and climate data. *Ecological Applications, 15*, 954-969

Yoder, B.J., & Waring, R.H. (1994). The Normalized Difference Vegetation Index of Small Douglas-Fir Canopies with Varying Chlorophyll Concentrations. *Remote Sensing of Environment, 49*, 81-91

Zhang, Q., Xiao, X., Braswell, B., Linder, E., Ollinger, S., Smith, M.L., Jenkins, J.P., Baret, F., Richardson, A.D., Moore, B., & Minocha, R. (2006). Characterization of seasonal variation of forest canopy in a temperate deciduous broadleaf forest, using daily MODIS data *Remote Sens. Environ., 105*, 189-203

Zhang, Q.Y., Xiao, X.M., Braswell, B., Linder, E., Baret, F., & Moore, B. (2005). Estimating light absorption by chlorophyll, leaf and canopy in a deciduous broadleaf forest using MODIS data and a radiative transfer model. *Remote Sens. Environ., 99*, 357-371

List of abbreviations and acronyms

BERMS - Boreal Ecosystem Research and Monitoring Sites

BOREAS - BOReal Ecosystem-Atmosphere Study

BRDF - bidirectional reflectance distribution function

chl - chlorophyll

EVI - enhanced vegetation index

FAPAR - fraction of absorbed photosynthetically active radiation

FCRN - Fluxnet-Canada Research Network

LSWI - land surface water index

LUE - light use efficiency

MCMC - Markov Chain Monte Carlo

MODIS - MODerate resolution Imaging Spectroradiometer

NDVI - normalized difference vegetation index

SOA - the Southern Old Aspen tower site

Table 1. *Days of useable daily 5x5 MODIS observations over the Southern Old Aspen site (SOA) during 2001-2005 (n=76)*

Year	Day of Year (DOY)
2001 n=22	144, 153, 155, 185, 189, 190, 215, 216, 218, 222, 224, 228, 233, 236, 245, 247, 249, 258, 261, 265, 272, 278
2002 n=16	156, 174, 177, 179, 188, 190, 193, 197, 216, 232, 235, 236, 239, 241, 261, 268
2003 n=12	139, 145, 148, 155, 166, 168, 197, 214, 226, 230, 237, 246
2004 n=9	182, 199, 206, 207, 208, 212, 217, 226, 247
2005 n=17	121, 122, 123, 128, 132, 150, 160, 173, 196, 219, 233, 244, 245, 247, 249, 285, 287

Table 2. *A list of variables in the PROSAIL-2 model and the search ranges used for inversion.*

	Variable	Description	Unit	Search range
Biophysical /biochemical variables	PAI	Plant area index, i.e., leaf +stem area index	m^2/m^2	1 – 7.5
	SFRAC	Stem fraction		0 –1
	CF	Cover fraction: area of land covered by vegetation/total area of land		0.5 –1
	C_{ab}	Leaf photosynthetic pigments including chlorophyll a+b and carotenoids	$\mu g/cm^2$	0 – 150
	N	Leaf structure variable: measure of the internal structure of the leaf		1.0 – 4.5
	C_w	Leaf equivalent water thickness	cm	0.001 – 0.15
	C_m	Leaf dry matter content	g/cm^2	0.001 – 0.04
	C_{brown}	Leaf brown pigment content		0.00001 – 8
	LFINC	Mean leaf inclination angle	degree	10 – 89
	STINC	Mean stem inclination angle	degree	10 – 89
	LFHOT	Leaf BRDF variable: length of leaf/ height of vegetation canopy		0 – 0.9
	STHOT	Stem BRDF variable: length of stem/ height of vegetation canopy		0 – 0.9
	$STEM_A$	Stem reflectance variable		0.0 – 1.0
	$BACK_A$	Background reflectance variable		0.0 – 1.0

Table 3. *Median values for photosynthetic pigments, water content, and dry matter at the grid cell level. LAI, CF, $FAPAR_{canopy}$ and $FAPAR_{chl}$ were estimated using PROSAIL-2 from daily 5x5 MODIS observations over the Southern Old Aspen site (SOA) in 2005. Note that the grid cell estimate = leaf level estimate*LAI*CF (where "estimate" refers to either photosynthetic pigments, water content, or dry matter, respectively)*

DOY in 2005	LAI	CF	Photosynthetic pigment ($\mu g/cm^2$)	Water content (cm)	Dry matter (g/cm^2)	$FAPAR_{canopy}$ 0-1	$FAPAR_{chl}$ 0-1
132	0.27	0.60	3.75	0.0005	0.0004	0.470	0.030
150	1.45	1.00	45.19	0.0050	0.0107	0.627	0.363
160	3.30	1.00	103.07	0.0311	0.0454	0.796	0.529
173	2.87	0.96	159.73	0.0326	0.0365	0.775	0.674
196	3.41	0.95	188.30	0.0345	0.0381	0.805	0.703
219	3.89	0.94	170.32	0.0385	0.0459	0.816	0.659
233	3.83	0.97	148.91	0.0417	0.0472	0.872	0.601
247	2.73	0.99	121.08	0.0450	0.0548	0.853	0.497
285	0.10	0.86	2.55	0.0005	0.0004	0.650	0.034

Table 4. *Annual averages (152≤ DOY≤ 259) of the median grid cell values of LAI, CF, photosynthetic pigment concentration, $FAPAR_{canopy}$, $FAPAR_{chl}$, LUE_{canopy} and LUE_{chl} for the area around the Old Aspen flux site.*

Year	LAI	CF	Photosynthetic pigment ($\mu g/cm^2$)	$FAPAR_{canopy}$ 0-1	$FAPAR_{chl}$ 0-1	LUE_{canopy} (μ mol C μ mol^{-1}PPFD)	LUE_{chl} (μ mol C μ mol^{-1}PPFD)
2001	3.49	0.98	175.73	0.856	0.652	0.0183	0.0242
2002	3.35	0.96	161.32	0.815	0.617	0.0183	0.0245
2003	3.23	0.94	123.68	0.794	0.582	0.0163	0.0225
2004	3.54	0.96	140.32	0.811	0.623	0.0244	0.0310
2005	3.14	0.97	135.56	0.820	0.589	0.0192	0.0267

Figure Captions

Fig. 1. Nadir MODIS NIR_1 reflectances (VZA < 5^0) for the 5 x 5 area (2.5 km x 2.5 km) on DOY 224 in 2001. The central grid cell covers the Southern Old Aspen [SOA] tower site in Canada.

Fig. 2. The relationship of $APAR_{chl}$ = [(90 min PPFD)*$FAPAR_{chl}$] to $APAR_{canopy}$ = [(90 min PPFD)*$FAPAR_{canopy}$] for 2001-2005. Solid diamonds (♦) indicate values retrieved during the core growing season (DOY:152-259; r = 0.87; $APAR_{chl}$ = 0.713 *$APAR_{canopy}$). Early (DOY<152) and late (DOY>259) season values were combined and are indicated with open triangles (Δ) (r = 0.55; $APAR_{chl}$ = 0.339* $APAR_{canopy}$). For all values (dashed line), r = 0.72 and $APAR_{chl}$ = 0.649*$APAR_{canopy}$.

Fig. 3. The relationship of GEP to $APAR_{canopy}$ = [(90 min PPFD)*$FAPAR_{canopy}$] in 2001-2005. Solid diamonds (♦) are data from during the core growing season (DOY 152-259). Open triangles (Δ) indicate values obtained before (DOY<152) or after (DOY>259). The apparent LUE_{canopy}, the slope of the relationship (0.0155 μmol C μmol^{-1} PPFD, r^2 = 0.33), is similar to the core growing season value (0.0173) but is considerably higher than for days having low GEP in the spring and fall.

Fig. 4. The relationship of GEP to $APAR_{chl}$ = [(90 min PPFD)*$FAPAR_{chl}$] in 2001-2005. Solid diamonds (♦) are data from during the core growing season (DOY 152-259, GEP = 0.0243*$APAR_{chl}$, r^2 = 0.63). Open triangles (Δ) indicate values obtained before (DOY<152) or

after (DOY>259) (GEP = 0.0208*$APAR_{chl}$, $r^2 = 0.64$). The apparent LUE_{chl}, i.e., the slope of the relationship for all values, is 0.0241 μmol C μmol^{-1} PPFD ($r^2 = 0.78$).

Fig. 5. Comparison of the annual means ± SE for $APAR_{chl}$ (♦) and $APAR_{canopy}$ (□) during the five-year period (2001-2005) for the growing season between DOY=152-259. $APAR_{chl}$ was significantly lower than $APAR_{canopy}$ in every year, averaging 235 μmol PPFD $m^{-2}s^{-1}$ less than $APAR_{canopy}$. $APAR_{tower}$ is not included in this figure because unlike $APAR_{chl}$ and $APAR_{canopy}$, it was obtained under all sky conditions, i.e., both clear and cloudy.

Fig. 6. Comparison of the annual means ± SE for MODIS-derived LUE_{chl} (♦) and LUE_{canopy} (□) during the five-year period (2001-2005) for the core growing season between DOY =152-259. LUE_{chl} was significantly higher than LUE_{canopy} in every year, averaging 0.007 μmol C μmol^{-1} PPFD higher. Annual LUE_{tower} values (Krishnan *et al.*, 2006) (Δ) agree well with our LUE_{chl}, falling within the SE range in 4 of 5 years. The maximum LUE (ε_{max}) for broadleaf forests used by the MODIS PSN model is shown as a horizontal dashed line.

Fig. 7. Linear relationship between annual average LUE as a function of the cumulative precipitation for the core growing season (DOY=152–259) in 2001-2005.

0.2112	0.2614	0.271	0.3094	0.2589
0.2916	0.3198	0.3079	0.3292	0.3335
0.3198	0.3294	0.338	0.3382	0.2982
0.3342	0.3318	0.2683	0.2982	0.2738
0.3211	0.2683	0.301	0.2784	0.1331

Fig. 1. Nadir MODIS NIR_1 reflectances (VZA < 5^0) for the 5 x 5 area (2.5 km x 2.5 km) on DOY 224 in 2001. The central grid cell covers the Southern Old Aspen [SOA] tower site in Canada.

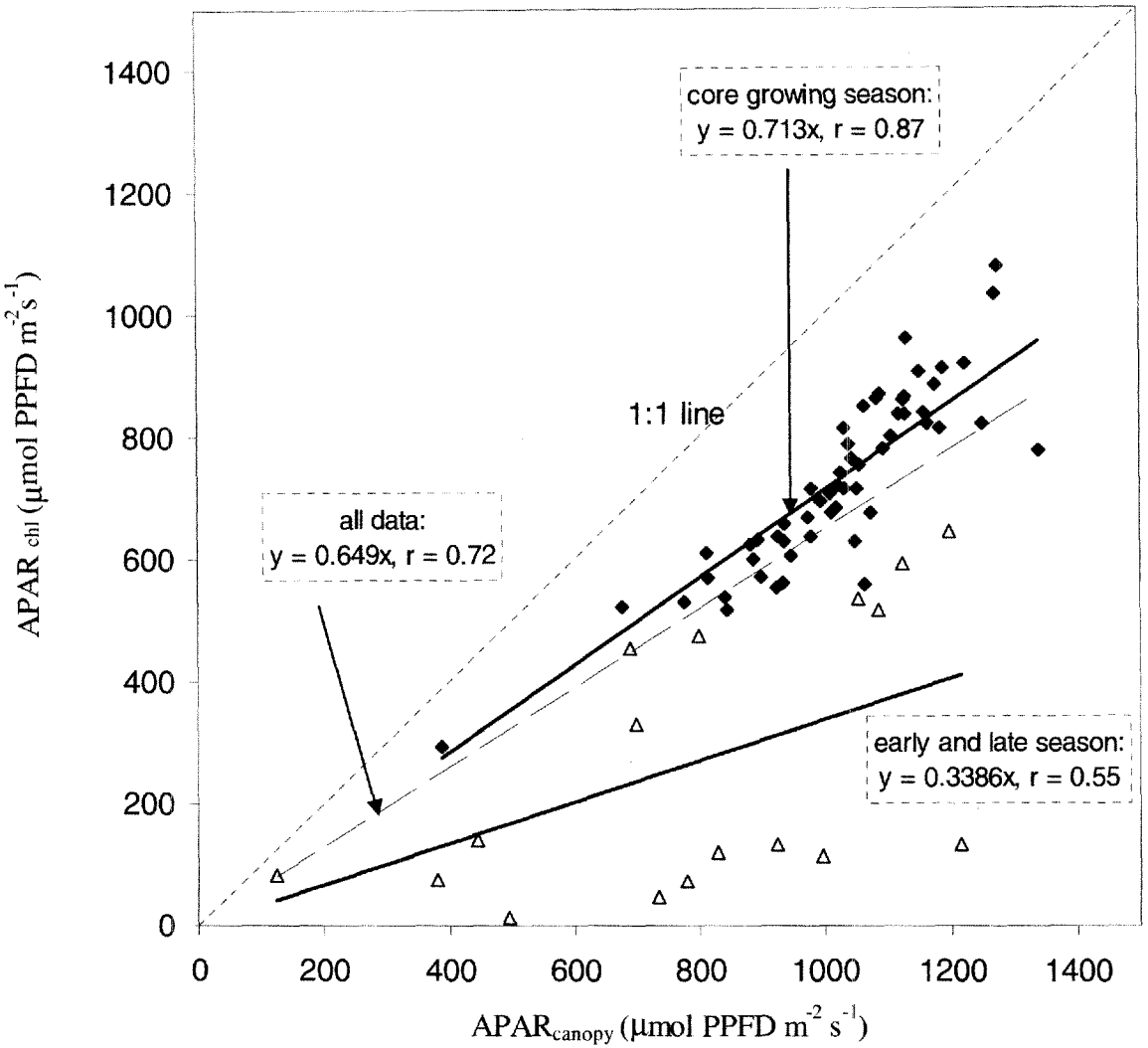

Fig. 2. The relationship of $APAR_{chl}$ = [(90 min PPFD)*$FAPAR_{chl}$] to $APAR_{canopy}$ = [(90 min PPFD)*$FAPAR_{canopy}$] for 2001-2005. Solid diamonds (♦) indicate values retrieved during the core growing season (DOY:152-259; r = 0.87; $APAR_{chl}$ = 0.713 *$APAR_{canopy}$). Early (DOY<152) and late (DOY>259) season values were combined and are indicated with open triangles (Δ) (r = 0.55; $APAR_{chl}$ = 0.339* $APAR_{canopy}$). For all values (dashed line), r = 0.72 and $APAR_{chl}$ = 0.649*$APAR_{canopy}$.

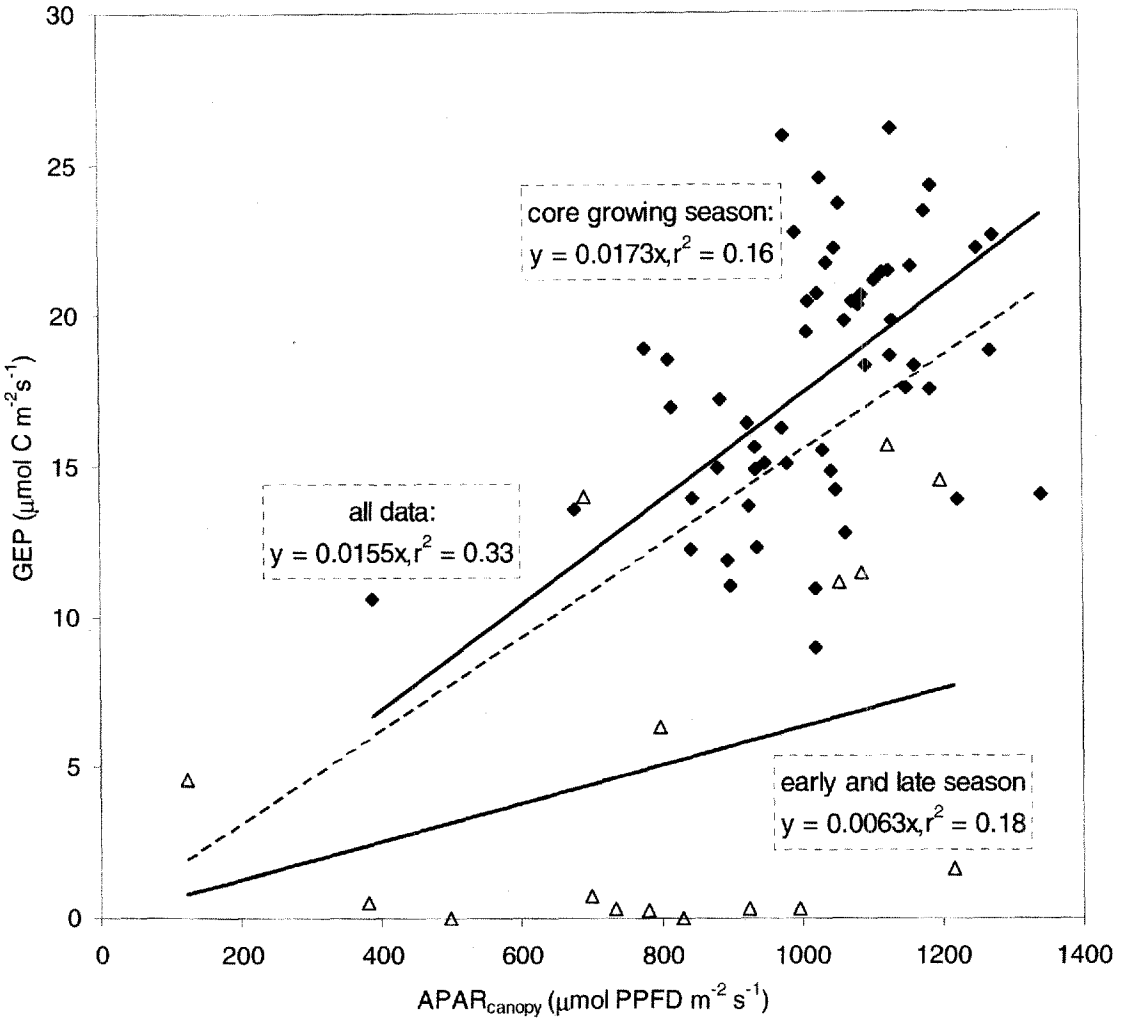

Fig. 3. The relationship of GEP to $APAR_{canopy}$ = [(90 min PPFD)*$FAPAR_{canopy}$] in 2001-2005. Solid diamonds (♦) are data from during the core growing season (DOY 152-259,GEP=0.0173*$APAR_{canopy}$,r^2=0.16). Open triangles (Δ) indicate values obtained before (DOY<152) or after (DOY>259)(GEP=0.0063*$APAR_{canopy}$,r^2=0.18). The apparent LUE_{canopy}, the slope of the relationship (0.0155 µmol C mmol-1 PPFD, r^2 = 0.33), is similar to the core growing season value (0.0173) but is considerably higher than for days having low GEP in the spring and fall.

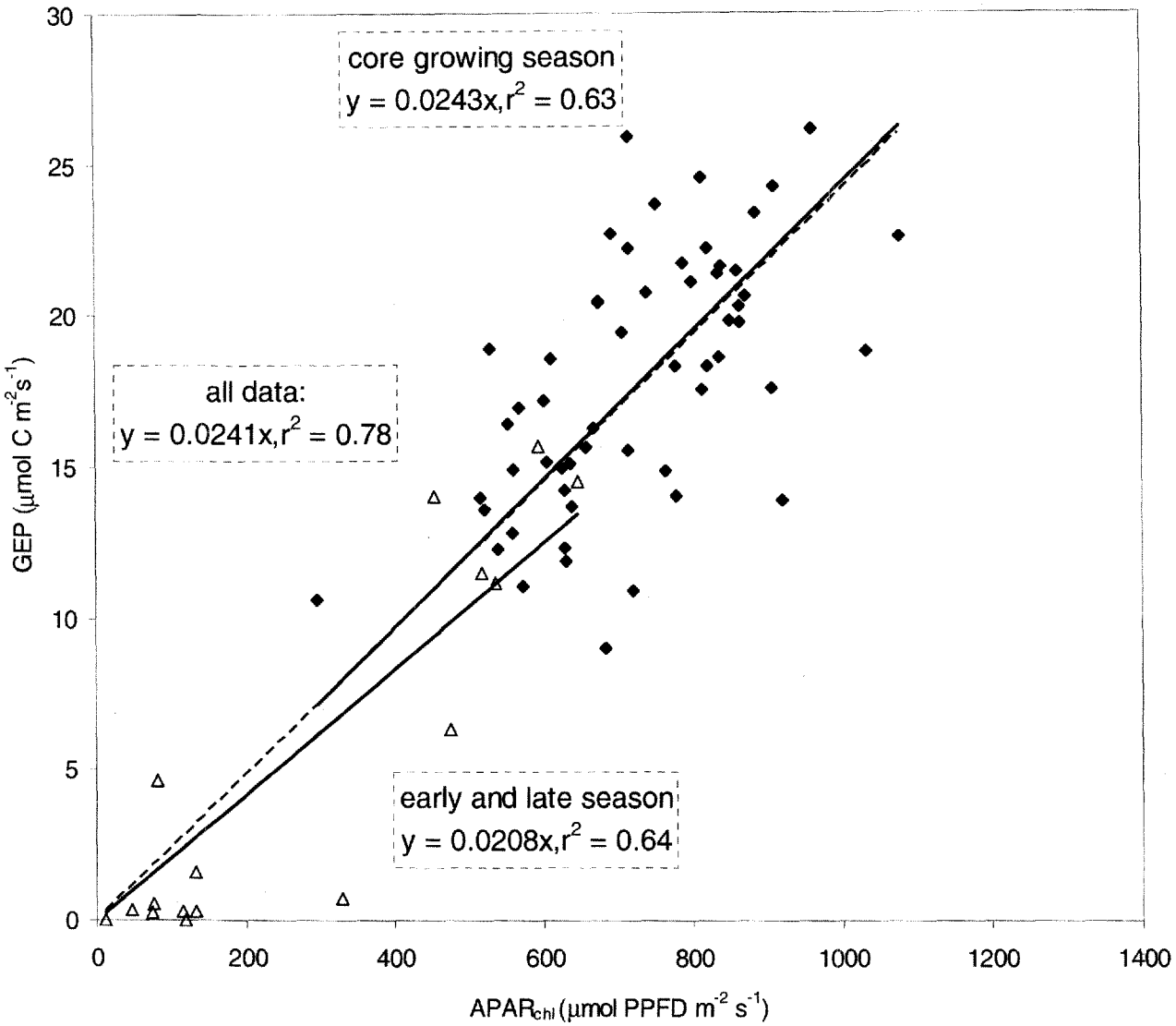

Fig. 4. The relationship of GEP to $APAR_{chl}$ = [(90 min PPFD)*$FAPAR_{chl}$] in 2001-2005. Solid diamonds (♦) are data from during the core growing season (DOY 152-259, GEP = 0.0243*$APAR_{chl}$, r^2 = 0.63). Open triangles (Δ) indicate values obtained before (DOY<152) or after (DOY>259) (GEP = 0.0208*$APAR_{chl}$, r^2 = 0.64). The apparent LUE_{chl}, i.e., the slope of the relationship for all values, is 0.0241 µmol C µmol-1 PPFD (r^2 = 0.78).

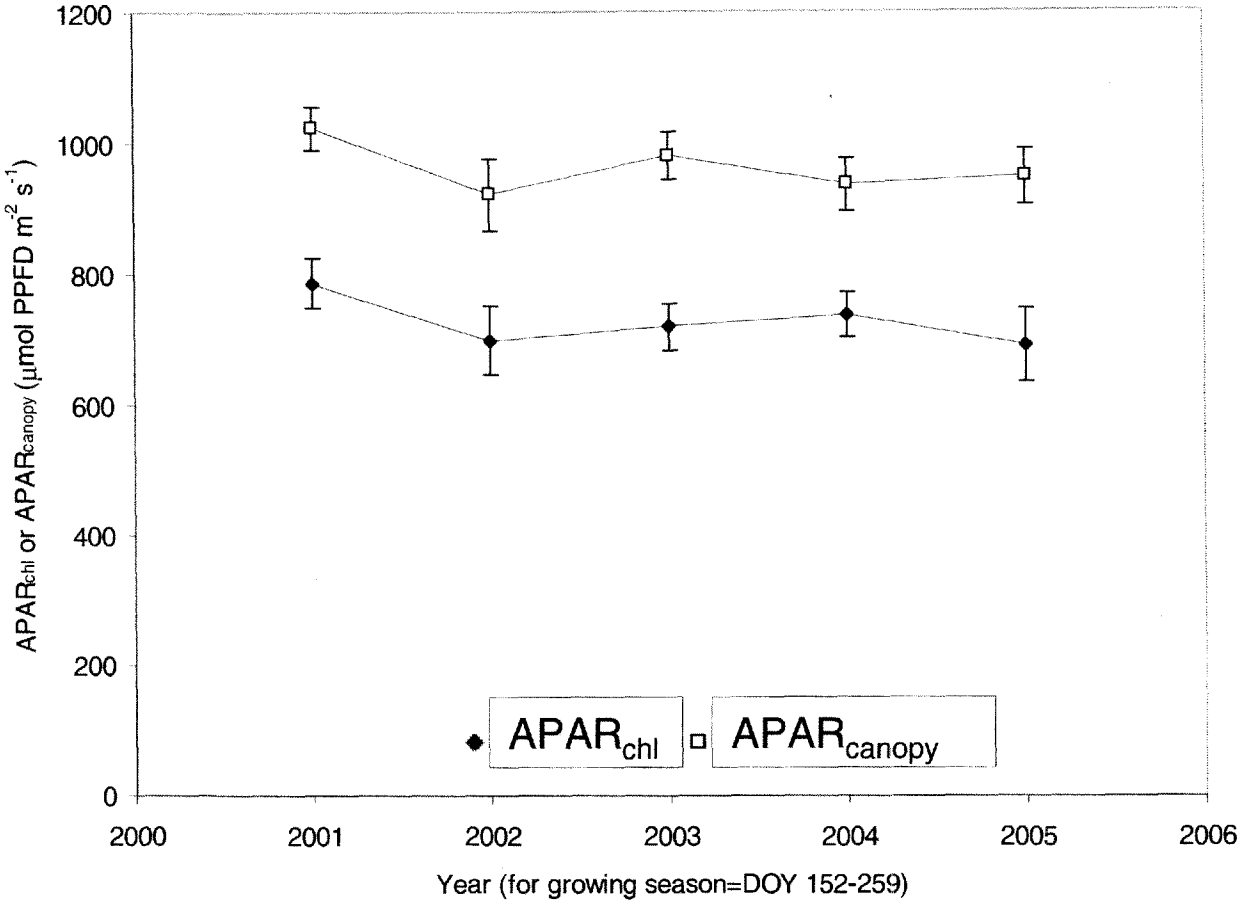

Fig. 5. Comparison of the annual means ± SE for $APAR_{chl}$ (♦) and $APAR_{canopy}$ (□) during the five-year period (2001-2005) for the growing season between DOY=152-259. $APAR_{chl}$ was significantly lower than $APAR_{canopy}$ in every year, averaging 235 µmol PPFD m^{-2} s^{-1} less than $APAR_{canopy}$. $APAR_{tower}$ is not included in this figure because unlike $APAR_{chl}$ and $APAR_{canopy}$, it was obtained under all sky conditions, i.e., both clear and cloudy.

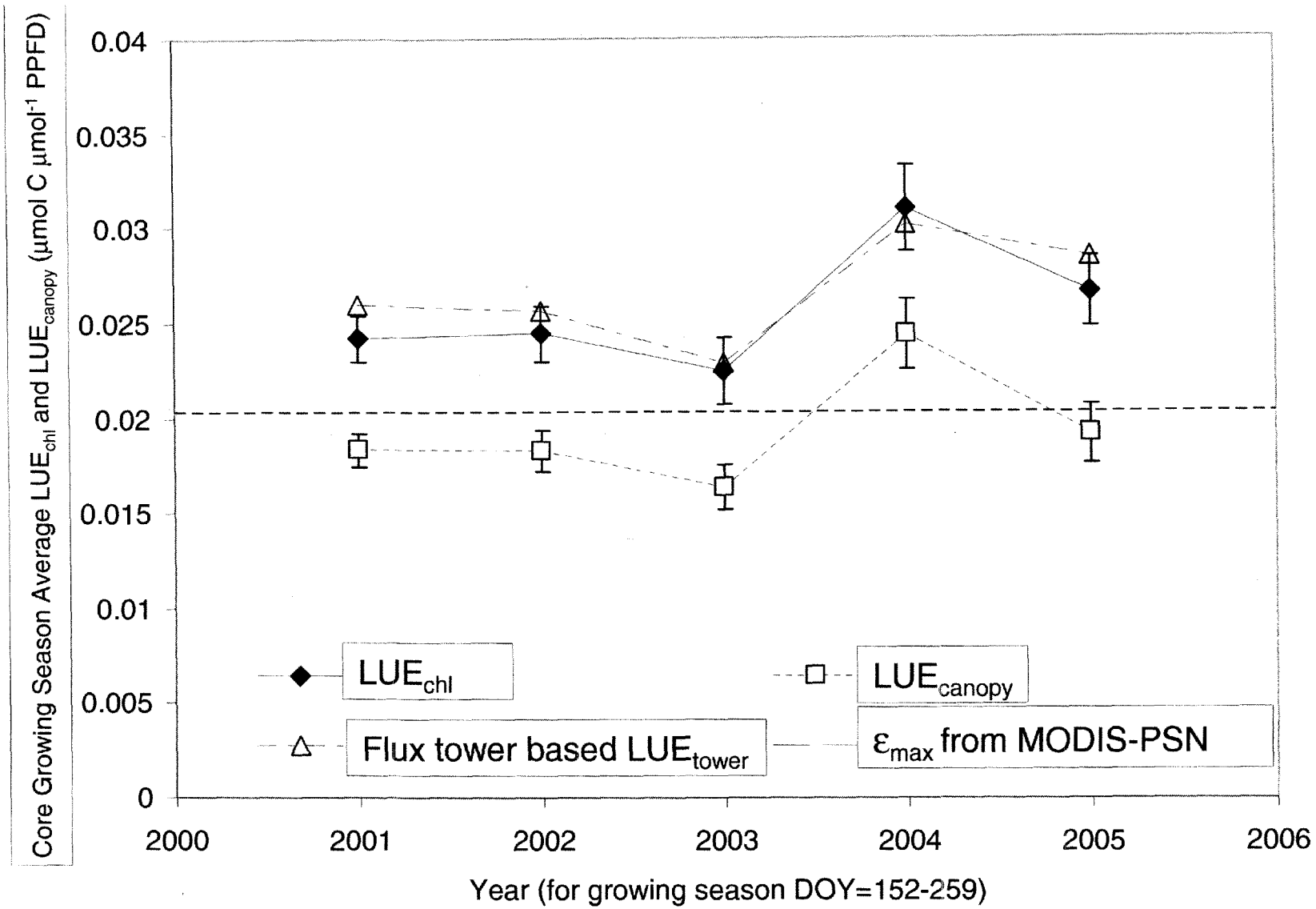

Fig. 6. Comparison of the annual means ± SE for MODIS-derived LUE$_{chl}$ (♦) and LUE$_{canopy}$ (□) during the five-year period (2001-2005) for the core growing season between DOY =152-259. LUE$_{chl}$ was significantly higher than LUE$_{canopy}$ in every year, averaging 0.007 µmol C µmol^{-1} PPFD higher. Annual LUE$_{tower}$ values (Krishnan *et al.*, 2006) (Δ) agree well with our LUE$_{chl}$, falling within the SE range in 4 of 5 years. The maximum LUE (ε_{max}) used by the MODIS-PSN model is shown as a horizontal dashed line(---).

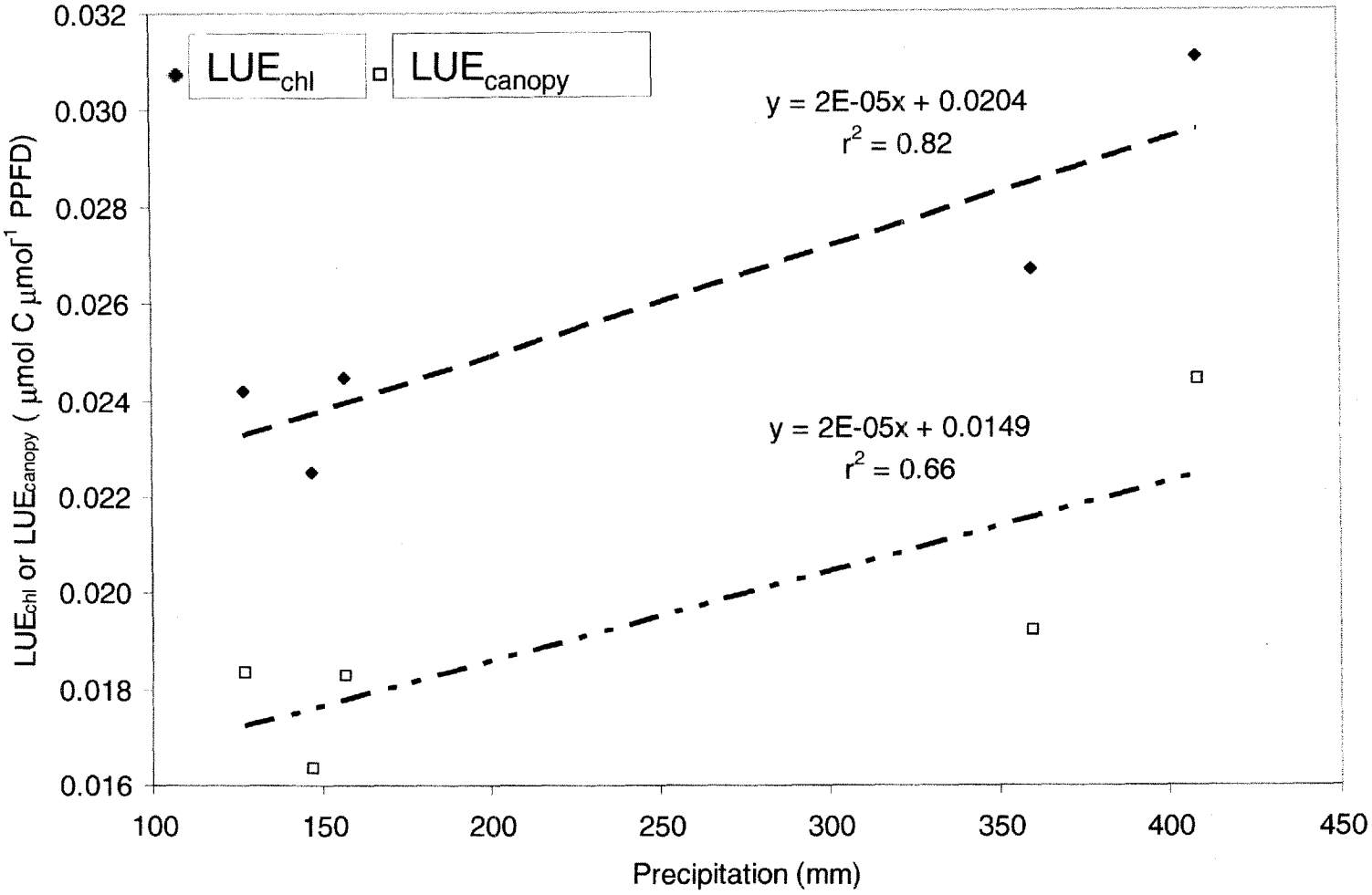

Fig. 7 Linear relationship between annual average LUE as a function of the cumulative precipitation for the core growing season (DOY=152–259) in 2001-2005.